Computer Assisted Mechanics and Engineering Sciences, 4: 327–344, 1997.

Aspects of Trefftz' Method in BEM and FEM and their coupling

Ulrich Brink
Institute for Structural and Computational Mechanics, University of Hannover, Appelstrasse 9A, D-30167 Hannover, Germany

Monika Kreienmeyer
Bundesanstalt für Geowissenschaften und Rohstoffe, Stilleweg 2, 30655 Hannover

Klaus Peters
Büro Dr. Schippke und Partner, Hildesheimer Str. 15, 30169 Hannover

Erwin Stein
Institute for Structural and Computational Mechanics, University of Hannover, Appelstrasse 9A, D-30167 Hannover, Germany

(Received December 20, 1996)

In both boundary element methods and Trefftz-type finite element methods a partial differential equation in some domain is treated by solving a discrete problem on the boundary of the domain and possibly the boundaries between subdomains. We consider a Trefftz element formulation which is based on the complementary energy functional, and we compare different regularizations of the interelement continuity conditions. Also starting from the complementary energy functional, mixed finite elements can be constructed such that the stresses satisfy equilibrium a priori. We describe a coupling of these elements with the by now classical symmetric Galerkin-BEM.

1. Introduction

Trefftz' method from the year 1926 [30] as well as the dual Ritz method from the year 1909 for the approximate solution of elliptic boundary value problems of second order are in case of more complicated domains and boundaries feasible and efficient only if test and trial functions in finite subdomains — finite elements — are introduced for treating direct or discrete variational problems. This is the reason why only much later, namely since 1943 by R. Courant and then 1956 by the engineers M. J. Turner, R. W. Clough, H. C. Martin and L. J. Topp the idea of discrete variational calculus could begin its great career in the form of the Finite Element Method (FEM), a Ritz or Galerkin method with finite subdomains. This career was enabled and amplified by the fast growth of electronic computer technology. There is of course a big mathematical step from Ritz' and Galerkin's original work to FEM because Sobolev spaces are needed for the test functions of finite elements fulfilling only weak differentiability conditions at the interelement boundaries. The convergence theory and especially the error analysis for adaptive FEM is more complicated than for the original Ritz and Galerkin method.

Trefftz' method did not have a similar strong development like FEM directly, but in an indirect sense the boundary integral equation method (BIEM or simply BEM) with test and trial functions for boundary elements became competitive in the 1980s and can also be understood as a Trefftz method in principle, using the singular fundamental solution in the Green–Gauss formula in order to obtain boundary integral equations. But it is of course possible to realize the idea of Trefftz' direct variational method for the approximation of boundary conditions, too. There is however the problem of regularization of non-conformities between the chosen field functions (represented as displacement or stress functions and fulfilling the differential equations) and the Trefftz Ansatz functions at the boundaries. Therefore hybrid-type Trefftz methods were proposed by different authors [15, 20, 22, 26, 33].

Unlike Ritz' method, Trefftz' method cannot easily be extended to partial differential equations of fourth order like the biharmonic Kirchhoff plate equation or the corresponding Kirchhoff–Love shell equations. In general consistency of the approximated displacements can only be achieved by at least one additional least square term at the boundaries [25, 31]. The important research work by Jirousek, Zielinski, Herrera, Piltner and Feixeira de Freitas over the past ten years showed the frontiers of enhanced Finite-Trefftz-Element methods. We believe that also [20] contributed to this state of the art.

Another field of applications of Trefftz' idea can be seen in the development of sophisticated mixed finite elements, especially based on the dual Hellinger–Reissner variational functional, aiming at equal convergence orders for displacements and stresses. The first element of this type was Pian's so-called hybrid stress element [21]. Over the last two decades rather complicated so-called dual mixed elements were developed with ansatz functions for the stresses lying in $H(\mathrm{div}, .)$-spaces, such as the PEERS element [2] and the BDM-element of Stenberg [29], for which a posteriori error analysis for adaptive mesh control was given in [3] and further applications in [5, 17]. The idea behind these elements is an optimal balance of trial functions for displacements and stresses in order to get improved convergence orders for the stresses and to guarantee stability in the sense of the Ladyzenskaya–Babuška–Brezzi condition. The conformity of the stresses is most conveniently achieved by Lagrange multipliers on the element boundaries, i.e. by a hybrid technique. We will comment on the relation between Trefftz' idea and these elements. They arise from extended variational functionals in order to fulfill consistency and stability requirements, which leads to quasioptimal convergence and robustness, namely insensitivity against changes of model and element parameters.

Another feature of Trefftz' method can be seen in recent error estimators for FEM using a postprocessing to get improved boundary tractions. This idea was also used by Ladeveze and treated in [27] in this volume.

In total, many sophisticated methods in BEM, FEM and coupled methods use Trefftz' idea, but hybrid and mixed regularization of the "dual Ritz problem" are necessary in order to get proper and competitive methods.

2. Aspects of Trefftz's idea in BEM formulations

The basic idea of the Trefftz method presented in 1926 [30] as an alternative to the Ritz method is the use of trial functions which satisfy a priori the governing differential equation. Substituting these trial functions into the according variational principle leads to an expression which contains only boundary integrals. This integral equation is discretized and solved for the boundary unknowns like in conventional boundary element algorithms.

The Trefftz formulations can be classified into the direct and the indirect formulations, and a similar classification is used for boundary element methods. In this section, we will briefly summarize the relations of Trefftz methods as *boundary-type* methods and standard boundary element methods. A comparison of Trefftz methods with BEM can be found in [16].

2.1. Direct methods

We consider the two-dimensional linear elasticity problem in a domain $\mathcal{B}_B$. A free energy function is postulated in the form

$$\Psi = \tfrac{1}{2}\varepsilon : \mathbb{C}\varepsilon \,, \tag{1}$$

with the elastic strains $\boldsymbol{\varepsilon} = \frac{1}{2}(\nabla \mathbf{u} + (\nabla \mathbf{u})^{\mathrm{T}})$ and the symmetric and positive definite elastic tensor $\mathbb{C}$. Then the stresses follow as

$$\boldsymbol{\sigma} = \partial_{\varepsilon}\Psi(\boldsymbol{\varepsilon}) = \mathbb{C}\boldsymbol{\varepsilon}. \tag{2}$$

In the direct BEM, we start from Kelvin's fundamental solution which for plane strain reads

$$\mathbf{G}\,(\mathbf{x},\mathbf{y}) = \frac{-1}{8\pi(1-\nu)G}\{(3-4\nu)\ln(r)\delta_{ij} - r_{,i}r_{,j}\} \tag{3}$$

with

$$r_i = \mathbf{y}_i - \mathbf{x}_i, \quad r = \sqrt{\langle r_i, r_i\rangle} = |\mathbf{y}-\mathbf{x}|, \quad r_{,i} = \frac{r_i}{r}.$$

G is the shear modulus and ν is Poisson's ratio. The traction on the boundary Γ_B of the BEM domain is denoted by $\mathbf{t}(\mathbf{y}) = \mathbf{T}_y\mathbf{u}(\mathbf{y})$. For simplicity we assume vanishing body loads. The displacements at any interior point of $\mathcal{B}_B$ are given by the Betti formula

$$\mathbf{u}(\mathbf{x}) = \int_{\Gamma_B} \mathbf{G}\,(\mathbf{x},\mathbf{y})\,\mathbf{t}(\mathbf{y})\,ds(\mathbf{y}) - \int_{\Gamma_B} (\mathbf{T}_y\mathbf{G}\,(\mathbf{x},\mathbf{y}))^{\mathrm{T}}\mathbf{u}(\mathbf{y})ds(\mathbf{y}), \tag{4}$$

where the traction operator $\mathbf{T}_y$ is applied columnwise to $\mathbf{G}$. Taking the limit $\mathbf{x} \to \Gamma_B$ we obtain the boundary integral equation [18]

$$\tfrac{1}{2}\mathbf{u} = \mathbf{V}\mathbf{t} - \mathbf{K}\mathbf{u}\,. \tag{5}$$

Here,

$$(\mathbf{V}\mathbf{t})(\mathbf{x}) := \int_{\Gamma_B} \mathbf{G}(\mathbf{x},\mathbf{y})\,\mathbf{t}(\mathbf{y})\,ds(\mathbf{y})\,, \qquad \mathbf{x} \in \Gamma_B\,,$$

is an integral operator with logarithmic singularity and

$$(\mathbf{K}\mathbf{u})(\mathbf{x}) := \int_{\Gamma_B} (\mathbf{T}_y\mathbf{G}(\mathbf{x},\mathbf{y}))^{\mathrm{T}}\,\mathbf{u}(\mathbf{y})\,ds(\mathbf{y})\,, \quad \mathbf{x} \in \Gamma_B,$$

is Cauchy singular. Applying the traction operator $\mathbf{T}_x$ we get another boundary integral equation

$$\tfrac{1}{2}\mathbf{t} = \mathbf{K}'\mathbf{t} - \mathbf{W}\mathbf{u} \tag{6}$$

with the adjoint of $\mathbf{K}$,

$$(\mathbf{K}'\mathbf{t})(\mathbf{x}) := \int_{\Gamma_B} \mathbf{T}_x\mathbf{G}(\mathbf{x},\mathbf{y})\,\mathbf{t}(\mathbf{y})\,ds(\mathbf{y})\,, \qquad \mathbf{x} \in \Gamma_B\,,$$

and the hypersingular integral operator

$$(\mathbf{W}\mathbf{u})(\mathbf{x}) := \mathbf{T}_x \int_{\Gamma_B} (\mathbf{T}_y\mathbf{G}(\mathbf{x},\mathbf{y}))^{\mathrm{T}}\,\mathbf{u}(\mathbf{y})\,ds(\mathbf{y})\,, \quad \mathbf{x} \in \Gamma_B\,.$$

In the above direct boundary integral formulation the singular fundamental solution is taken as a weight function. On the other hand, in the direct Trefftz formulation, the regular T-complete function (see [13]) which satisfies the governing equations is taken as the weight function. The direct Trefftz method was first presented by Cheung et al. [8] for the two-dimensional potential problem and extended to more complex problems like linear elasticity in [14].

Boundary element methods and the direct Trefftz method lead to boundary integral equations which can be solved by different numerical methods, among them collocation, Bubnov–Galerkin, Nyström and least-square method. All of them lead to a fully populated system matrix which is nonsymmetric in the case of collocation and symmetric but in general indefinite if a Bubnov–Galerkin method with both integral equations is used. For this reason, special iterative solvers for nonsymmetric and/or indefinite linear systems of equations should be used.

2.2. Indirect methods

In the indirect formulation, the solution of the problem is approximated by the superposition of functions satisfying the governing equation. The unknowns are then determined so that the approximate solution satisfies the boundary conditions either in some special points (collocation method) or in an integral sense (Galerkin method, least-square method). Obviously, the original Trefftz method [30] can be classified as an indirect method. In the field of elastic analysis, the so-called *singularity method* was first presented by Kupradze [18] in 1965. This method is identical to the indirect boundary element method which is much less used in engineering computations than the direct one.

Another indirect method is the *modified* Trefftz method by Patterson and Sheikh [19] and Oliviera [1]. In this formulation, the approximate solution is represented by the linear combination of the singular fundamental solution. This method is basically identical to the indirect boundary element method based on the regular integral equation.

It follows that the Trefftz method and the boundary element method have very close connections. The direct Trefftz method can be seen as the direct boundary element method formulated by introducing T-complete functions instead of fundamental solutions. The main common aspect is Trefftz's idea of using ansatz functions satisfying the governing equations; this leads to a boundary integral equation which can be solved by the above mentioned numerical methods.

3. TREFFTZ-TYPE FINITE ELEMENTS

3.1. Boundary-type finite elements

Starting from the variational principle with the so-called hybrid stress method the trial functions for the stresses have to fulfill the *Beltrami*-equations, that means also the compatibility equations for the strains. So the divergence theorem can be applied, and one arrives at a pure boundary formulation in the sense of *Trefftz*'s method. Beside the resulting variational formulation different regularizations of the interelement conditions are chosen.

3.1.1. Functional and regularization

The complementary energy functional for a body $\mathcal{B}$ which is discretized into n elements $\mathcal{B}_e \subset \mathbb{R}^2$ is given by

$$\overset{*}{\pi}_h = \frac{1}{2}\int_{\cup\mathcal{B}_e} \boldsymbol{\sigma}_h^T \mathbf{C}^{-1} \boldsymbol{\sigma}_h d\mathbf{x} + \pi_a \rightarrow \min . \tag{7}$$

The Treffz elements are based on the introduction of shape functions for the stresses $\boldsymbol{\sigma}_h$ which fulfill the homogeneous differential equations $\triangle\triangle\boldsymbol{\sigma}_h = \mathbf{0}$, but not the boundary conditions. The related strains $\boldsymbol{\varepsilon}(\boldsymbol{\sigma}_h)$ in $\mathcal{B}$ are integrable and the displacements $\mathbf{u}_h(\boldsymbol{\sigma}_h)$ can be derived.

With the shape functions $\mathbf{N}_\sigma$, the stresses are defined by

$$\boldsymbol{\sigma}_h = \mathbf{N}_\sigma \boldsymbol{\beta} \quad \text{in} \quad \mathcal{B}_e. \tag{8}$$

With the material law and the integrability conditions, we obtain

$$\begin{aligned} \boldsymbol{\varepsilon}_h(\boldsymbol{\sigma}_h) &= \mathbf{C}^{-1}\mathbf{N}_\sigma \boldsymbol{\beta} && \text{in} \quad \mathcal{B}_e \cup \Gamma_e , \\ \mathbf{u}_h(\boldsymbol{\sigma}_h) &= \int_{[S]} \boldsymbol{\varepsilon}_h ds = \mathbf{Z}\boldsymbol{\beta} && \text{in} \quad \mathcal{B}_e \cup \Gamma_e , \\ \mathbf{t}_h(\boldsymbol{\sigma}_h) &= \mathcal{R}\boldsymbol{\sigma}_h = \mathcal{R}\mathbf{N}_\sigma \boldsymbol{\beta} = \mathcal{R}\boldsymbol{\beta} && \text{on} \quad \Gamma_e . \end{aligned} \tag{9}$$

The displacements $\bar{\mathbf{u}}_h$, defined on the surface Γ_e by the nodal displacement vector $\mathbf{v}$ as

$$\bar{\mathbf{u}}_h = \mathbf{N}_u \mathbf{v} \quad \text{on} \quad \Gamma_e \tag{10}$$

are used as an additional regularization for the interelement conditions.

The continuity of the boundary displacements at the nodes can be described by

$$J_K = \sum_{i=1}^{n} |\mathbf{u}_{hi}(\boldsymbol{\sigma}_h) - \bar{\mathbf{u}}_{hi}| \quad = 0 \qquad (\mathrm{K}), \tag{11}$$

or another type of continuity requirement is the least-squares method

$$J_F = \int_\Gamma [\mathbf{u}_h(\boldsymbol{\sigma}_h) - \bar{\mathbf{u}}_h]^2 \, \mathrm{d}s \quad \to \min \qquad (\mathrm{F}) \tag{12}$$

or other Lagrangian terms, see Reference [20].

The terms in equations (11) and (12) are nodal and weak coupling conditions of the Trefftz element domains for displacements or stresses, see Figure 1.

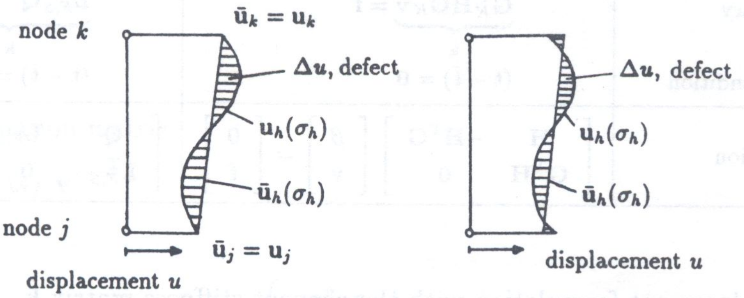

Fig. 1. Nodal and weak coupling of the displacements

Equation (11) postulates that the continuity of the natural boundary condition is fulfilled exactly in selected node points k at the interfaces of adjacent Trefftz elements via the interelement displacement functions $\bar{\mathbf{u}}_h$. This is a strong coupling condition for selected points.

Equation (12) postulates — in contrast to the first one — the minimization of the displacements $\mathbf{u}$ and $\bar{\mathbf{u}}$ in a quadratic average sense so that the defect on the surface is minimized. This is a regularization for the natural interface condition $\mathbf{u}^+ = \mathbf{u}^-$.

Table 1 shows the essential/natural and the remaining interface conditions for the different Trefftz formulations.

3.1.2. Element matrices, elimination of stress parameters

The complementary stress potential

$$\overset{*}{\pi}_i = \frac{1}{2} \int_{\cup \mathcal{B}_e} \boldsymbol{\sigma}_h^{\mathrm{T}} \mathbf{C}^{-1} \boldsymbol{\sigma}_h \, \mathrm{d}\mathbf{x} \tag{13}$$

can be written as the surface integral

$$\overset{*}{\pi}_i = \frac{1}{2} \int_{\Gamma_e} \mathbf{u}_h^{\mathrm{T}}(\boldsymbol{\sigma}_h) \mathbf{t}_h(\boldsymbol{\sigma}_h) \, \mathrm{d}s \tag{14}$$

because the static field equations are fulfilled by the trial function $\boldsymbol{\sigma}_h$.

From the symmetric quadratic form for the stress energy of an element

$$\overset{*}{\pi}_i = \tfrac{1}{2} \boldsymbol{\beta}^{\mathrm{T}} \mathbf{H} \boldsymbol{\beta} \tag{15}$$

we can derive the matrix $\mathbf{H}$ from equations (9) and (14)

$$\mathbf{H} = \frac{1}{2} \int_{\Gamma_e} \left(\mathbf{Z}^{\mathrm{T}} \mathbf{R} + \mathbf{R}^{\mathrm{T}} \mathbf{Z} \right) \mathrm{d}s = \mathbf{H}^{\mathrm{T}}. \tag{16}$$

Table 1. Essential and natural interface conditions for different Trefftz formulations

Trefftz formulation	Nodal displacement errors (K)	Squared error of displacements (F)
Method Internal complementary energy + constraints	$J_K = \sum_{i=1}^{n} \left\lvert \mathbf{u}^i - \bar{\mathbf{u}}^i \right\rvert = 0$	$J_F = \int_\Gamma (\mathbf{u} - \bar{\mathbf{u}})^2 \, \mathrm{d}\Gamma \to \min$
Total complementary energy $\varepsilon = \varepsilon(\sigma)$	$\pi_k = \frac{1}{2} \int_V \boldsymbol{\varepsilon}^{\mathrm{T}} \boldsymbol{\sigma} \, \mathrm{d}V - \int_\Gamma \mathbf{u}^{\mathrm{T}} \bar{\mathbf{t}} \, \mathrm{d}\Gamma$	$\pi_k = \frac{1}{2} \int_V \boldsymbol{\varepsilon}^{\mathrm{T}} \boldsymbol{\sigma} \, \mathrm{d}V - \int_\Gamma \mathbf{u}^{\mathrm{T}} \bar{\mathbf{t}} \, \mathrm{d}\Gamma$
Variation of the: Internal complementary energy + constraints (1) Essential interface condition	$\boldsymbol{\beta} = \mathbf{H}^{-1}\mathbf{H}^{\mathrm{T}}\mathbf{G}_K \mathbf{v} = \mathbf{G}_K \mathbf{v}$ $(\mathbf{u} - \bar{\mathbf{u}}) = \mathbf{0}$	$\boldsymbol{\beta} = \mathbf{Q}^{-1}\mathbf{L}_{F,S}\mathbf{v} = \mathbf{G}_{F,S}\mathbf{v}$ $(\mathbf{u} - \bar{\mathbf{u}}) = \mathbf{0}$
Total complementary energy (1) in (2) Natural interface condition	$\underbrace{\mathbf{G}_K^{\mathrm{T}}\mathbf{H}\mathbf{G}_K}_{\hat{\mathbf{k}}}\mathbf{v} = \mathbf{f}$ $(\mathbf{t} - \bar{\mathbf{t}}) = \mathbf{0}$	$\underbrace{\mathbf{L}_{F,S}^{\mathrm{T}}\mathbf{Q}^{-1}\mathbf{L}_{F,S}}_{\hat{\mathbf{k}}}\mathbf{v} = \mathbf{f}$ $(\mathbf{t} - \bar{\mathbf{t}}) = \mathbf{0}$
Matrix representation	$\begin{bmatrix} \mathbf{H} & -\mathbf{H}^{\mathrm{T}}\mathbf{G} \\ \mathbf{G}^{\mathrm{T}}\mathbf{H} & \mathbf{0} \end{bmatrix} \begin{bmatrix} \boldsymbol{\beta} \\ \mathbf{v} \end{bmatrix} = \begin{bmatrix} \mathbf{0} \\ \mathbf{f} \end{bmatrix}$	$\begin{bmatrix} \mathbf{Q} & -\mathbf{L}_{F,S} \\ \mathbf{L}_{F,S}^{\mathrm{T}} & \mathbf{0} \end{bmatrix} \begin{bmatrix} \boldsymbol{\beta} \\ \mathbf{v} \end{bmatrix} = \begin{bmatrix} \mathbf{0} \\ \mathbf{f} \end{bmatrix}$

To get a nodal displacement formulation with the element stiffness matrix $\hat{\mathbf{k}}$,

$$\pi_i = \tfrac{1}{2}\mathbf{v}^{\mathrm{T}}\hat{\mathbf{k}}\mathbf{v}, \tag{17}$$

one of the regularizations is used.

The transformation matrix $\mathbf{G}$ that connects the stress parameters $\boldsymbol{\beta}$ with the nodal displacements $\mathbf{v}$

$$\boldsymbol{\beta} = \mathbf{G}\mathbf{v} \tag{18}$$

is calculated as shown below. The order of the row regularity must correspond to the number of the independent stress parameters.

The Trefftz stiffness matrix is given by

$$\hat{\mathbf{k}} = \mathbf{G}^{\mathrm{T}}\,\mathbf{H}\,\mathbf{G}. \tag{19}$$

In the sequel the matrix $\mathbf{G}$ is derived for different terms.

From equation (11)

$$J_K = \sum_{(k)} \mid \mathbf{u}_h^k - \bar{\mathbf{u}}_h^k \mid = 0 \tag{20}$$

with the trial functions

$$\mathbf{u}_h^k = \mathbf{Z}^k\boldsymbol{\beta} \quad \text{in} \quad \mathcal{B}_e\,; \qquad \bar{\mathbf{u}}_h^k = \mathbf{N}_u^k\mathbf{v} \quad \text{on} \quad \Gamma_e \tag{21}$$

written for every node k

$$\begin{bmatrix} \mathbf{Z}^1 \\ \mathbf{Z}^2 \\ \vdots \\ \mathbf{Z}^k \end{bmatrix} \begin{bmatrix} \beta_1 \\ \beta_2 \\ \vdots \\ \beta_m \end{bmatrix} = \begin{bmatrix} \mathbf{H}_u^1 \\ \mathbf{H}_u^2 \\ \vdots \\ \mathbf{H}_u^k \end{bmatrix} \begin{bmatrix} \mathbf{v}^1 \\ \mathbf{v}^2 \\ \vdots \\ \mathbf{v}^k \end{bmatrix}$$

$$\mathbf{Z}_G\boldsymbol{\beta} = \mathbf{1v} \tag{22}$$

one obtains the transformation matrix $\mathbf{G}_K$

$$\boldsymbol{\beta} = \mathbf{Z}_G^{-1}\mathbf{v} = \mathbf{G}_K\mathbf{v}. \tag{23}$$

Equation (12)

$$J_F = \int_{\Gamma_e} (\mathbf{u}_h - \bar{\mathbf{u}}_h)^2 \, \mathrm{d}s \longrightarrow \min \tag{24}$$

with the trial functions

$$\mathbf{u}_h(\boldsymbol{\sigma}_h) = \mathbf{Z}\boldsymbol{\beta} \quad \text{in} \quad \mathcal{B}_e; \qquad \bar{\mathbf{u}}_h = \mathbf{N}_u\mathbf{v} \quad \text{on} \quad \Gamma_e \tag{25}$$

and the stationary condition

$$\frac{\partial J_F}{\partial \boldsymbol{\beta}} = 0 \tag{26}$$

yields the transformation matrix

$$\boldsymbol{\beta} = \mathbf{Q}_F^{-1}\mathbf{L}_F\mathbf{v} = \mathbf{G}_F\,\mathbf{v} \tag{27}$$

with

$$\mathbf{Q}_F = \int_{\Gamma_e} \mathbf{Z}^{\mathrm{T}}\mathbf{Z}\,\mathrm{d}s \qquad \text{and} \qquad \mathbf{L}_F = \int_{\Gamma_e} \mathbf{Z}^{\mathrm{T}}\mathbf{N}_u\,\mathrm{d}s. \tag{28}$$

3.1.3. Numerical integration, trial functions

The trial functions for the stresses can be gained from the stress tensor $\boldsymbol{\chi}$

$$\sigma = \mathrm{Ink}\,\chi = -e_{ijk}e_{rst}\chi_{kt,js} \tag{29}$$

and has to fulfill the *Beltrami*-equation

$$\mathrm{Ink}\left(\mathbf{C}^{-1}\,(\mathrm{Ink}\,\chi)\right) = 0. \tag{30}$$

This ensures that the equilibrium conditions, the constitutive law and the integrability conditions for the strains are fulfilled by the stress trial functions in the element domain.

Several solutions for isotropic and anisotropic elastic materials are found for 2d-problems where a characteristic equation has to be solved which is dependent on the constitutive law.

In this paper linear 2d-stress functions are shown which fulfill the homogeneous differential equation independent of the constitutive law:

$$\boldsymbol{\sigma}^{\mathrm{T}} = [\sigma_x\,\sigma_y\,\sigma_{xy}], \tag{31}$$

$$\mathbf{N}_\sigma = \begin{bmatrix} 1 & 0 & 0 & y & 0 \\ 0 & 1 & 0 & 0 & x \\ 0 & 0 & 1 & 0 & 0 \end{bmatrix}.$$

The computation of an element stiffness matrix is performed numerically with a surface integration technique, using the isoparametric projection.

In contrast to the conventional isoparametric concept, where the trial functions are defined first in the ξ, η-coordinate system of the unit surface and then are transformed into the real shape, the trial functions of the Trefftz elements are defined in the real element domain and then have to be integrated over the real element surfaces.

3.1.4. Example

A cantilever beam with a pure bending load is treated, using a distorted element mesh, see Figure 2. The results of the Trefftz element formulation are shown in Figure 3.

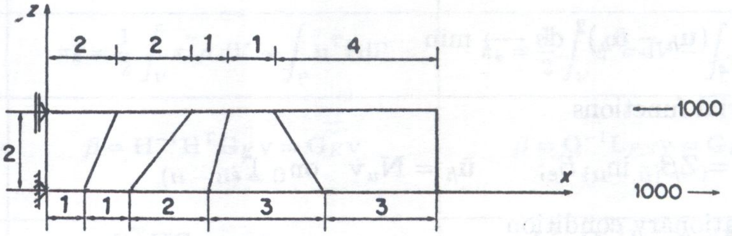

Fig. 2. System, load and discretization

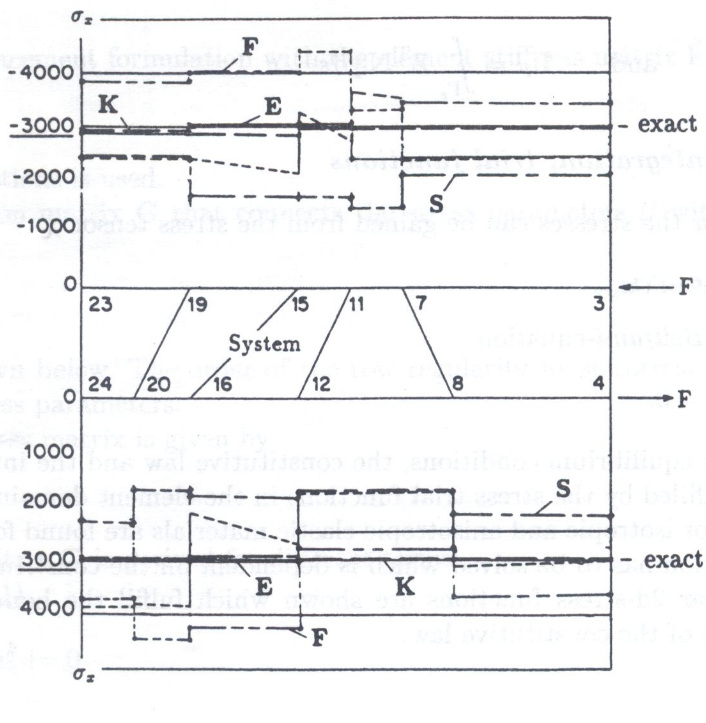

Fig. 3. Stresses σ_x at the top and the bottom of the beam

The following element formulations are used:

K, F see equations (11) and (12),

E, L S see Reference [20].

The nodal interelement condition (K) seems to be the most accurate formulation.

The Trefftz elements lead to more accurate results than other hybrid or displacement elements within the same order of shape functions.

3.2. Dual mixed elements satisfying equilibrium

Employing an extension of the complementary energy principle, it is possible to derive dual mixed finite elements such that the constraint $\operatorname{div}\boldsymbol{\sigma}_h = -\mathbf{f}$ is satisfied provided that the body loads $\mathbf{f}$ have sufficiently simple form. We consider the linear elasticity problem

$$\left.\begin{array}{ll} \operatorname{div}\boldsymbol{\sigma} = -\mathbf{f} & \text{in } \mathcal{B} \\ \boldsymbol{\sigma} - \mathbb{C}\varepsilon(\mathbf{u}) = \mathbf{0} & \text{in } \mathcal{B} \\ \mathbf{u} = \bar{\mathbf{u}} & \text{on } \Gamma_u \\ \boldsymbol{\sigma}\mathbf{n} = \bar{\mathbf{t}} & \text{on } \Gamma_t \end{array}\right\} \tag{32}$$

in a polygon domain $\mathcal{B} \subset \mathbb{R}^2$.

We start from the saddle point problem

$$\inf_{\boldsymbol{\sigma}\in\mathbf{H}(\operatorname{div},\mathcal{B})^{\text{sym}}} \ \sup_{\mathbf{u}\in\mathbf{L}_2(\mathcal{B})} \Pi(\boldsymbol{\sigma},\mathbf{u}), \tag{33}$$

with the functional

$$\Pi(\boldsymbol{\sigma},\mathbf{u}) := \frac{1}{2}\int_{\mathcal{B}_F} \boldsymbol{\sigma} : \mathbb{C}^{-1}\boldsymbol{\sigma}\,\mathrm{d}\mathcal{B} + \int_{\mathcal{B}_F} (\operatorname{div}\boldsymbol{\sigma} + \mathbf{f})\cdot\mathbf{u}\,\mathrm{d}\mathcal{B} - \int_{\Gamma_u} \boldsymbol{\sigma}\mathbf{n}\cdot\bar{\mathbf{u}}\,\mathrm{d}s\,.$$

Here the stresses are sought in the space

$$\mathbf{H}(\operatorname{div},\mathcal{B})^{\text{sym}} := \left\{\boldsymbol{\tau} \in L_2(\mathcal{B})^{2\times 2} : \operatorname{div}\boldsymbol{\tau} \in L_2(\mathcal{B})^2, \quad \boldsymbol{\tau} = \boldsymbol{\tau}^{\mathrm{T}}, \quad \boldsymbol{\tau}\mathbf{n} = \bar{\mathbf{t}} \ \text{ on } \ \Gamma_t\right\}. \tag{34}$$

In this formulation, $\mathbf{u} = \bar{\mathbf{u}}$ on Γ_u is a natural boundary condition.

It is not trivial to find stable finite element spaces for the discretization of the above saddle point problem. One approach is to relax the symmetry of the stress tensor. This means a Lagrange multiplier γ is introduced to ensure symmetry of $\boldsymbol{\sigma}$ in a weak form. The functional becomes

$$\tilde{\Pi}(\boldsymbol{\sigma},\mathbf{u},\gamma) := \Pi(\boldsymbol{\sigma},\mathbf{u}) + \int_{\mathcal{B}_F} \operatorname{as}(\boldsymbol{\sigma})\,\gamma\,\mathrm{d}\mathcal{B}$$

with $\operatorname{as}(\boldsymbol{\sigma}) := \sigma_{21} - \sigma_{12}$ being the asymmetric part of $\boldsymbol{\sigma}$. Now we seek the saddle point

$$\inf_{\boldsymbol{\sigma}\in\mathbf{H}(\operatorname{div},\mathcal{B})} \ \sup_{\mathbf{u}\in\mathbf{L}_2(\mathcal{B})} \ \sup_{\gamma\in\mathbf{L}_2(\mathcal{B})} \tilde{\Pi}(\boldsymbol{\sigma},\mathbf{u},\gamma). \tag{35}$$

The stresses are sought in the space $\mathbf{H}(\operatorname{div},\mathcal{B})$ as defined in (34), but with the condition $\boldsymbol{\tau} = \boldsymbol{\tau}^{\mathrm{T}}$ dropped. It can be shown that at the saddle point the Lagrange multiplier γ corresponds to the rotation, i.e.

$$\gamma = \tfrac{1}{2}\operatorname{rot}\mathbf{u} = \frac{1}{2}\left(\frac{\partial u_2}{\partial x} - \frac{\partial u_1}{\partial y}\right).$$

The weak formulation corresponding to (35) reads: Find $\boldsymbol{\sigma} \in \mathbf{H}(\operatorname{div},\mathcal{B})$, $\mathbf{u} \in L_2(\mathcal{B})$ and $\gamma \in L_2(\mathcal{B})$ such that

$$\begin{array}{ll} \displaystyle\int_{\mathcal{B}} \boldsymbol{\tau} : \mathbb{C}^{-1}\boldsymbol{\sigma}\,\mathrm{d}\mathcal{B} + \int_{\mathcal{B}} \operatorname{div}\boldsymbol{\tau}\cdot\mathbf{u}\,\mathrm{d}\mathcal{B} + \int_{\mathcal{B}} \operatorname{as}(\boldsymbol{\tau})\,\gamma\,\mathrm{d}\mathcal{B} = \int_{\Gamma_u} \boldsymbol{\tau}\mathbf{n}\cdot\bar{\mathbf{u}}\,\mathrm{d}s & \forall\boldsymbol{\tau}, \\ \displaystyle\int_{\mathcal{B}} \operatorname{div}\boldsymbol{\sigma}\cdot\mathbf{v}\,\mathrm{d}\mathcal{B} = -\int_{\mathcal{B}} \mathbf{f}\cdot\mathbf{v}\,\mathrm{d}\mathcal{B} & \forall\mathbf{v}\in L_2(\mathcal{B}), \\ \displaystyle\int_{\mathcal{B}} \operatorname{as}(\boldsymbol{\sigma})\,\theta\,\mathrm{d}\mathcal{B} = 0 & \forall\theta\in L_2(\mathcal{B}), \end{array} \tag{36}$$

where the test functions $\boldsymbol{\tau}$ satisfy $\boldsymbol{\tau} \in L_2(\mathcal{B})^{2\times 2}$, $\operatorname{div}\boldsymbol{\tau} \in L_2(\mathcal{B})^2$, and $\boldsymbol{\tau}\mathbf{n} = 0$ on Γ_t.

Next we describe finite element spaces, following Stenberg [29]. The FEM domain $\mathcal{B}$ is partitioned into triangles. Two different triangles share at most a common edge or a common vertex. For each triangle $\mathcal{B}_e$ we define a bubble function $b_e(\mathbf{x})$ of polynomial degree three which vanishes on the element boundary $\partial\mathcal{B}_e$. On the unit triangle with the vertices $(0,0)$, $(1,0)$, $(0,1)$ the bubble function is given by $b_0(\xi,\eta) = \xi\eta(1-\xi-\eta)$ in local coordinates (ξ,η). On each element $\mathcal{B}_e$, the stresses belong to the 15-dimensional space

$$\mathcal{S}(\mathcal{B}_e) := \operatorname{span}\left\{ \mathcal{P}_1(\mathcal{B}_e)^{2\times 2}, \begin{pmatrix} 0 & -b_e \\ b_e & 0 \end{pmatrix}, \begin{pmatrix} -\frac{\partial}{\partial y} b_e & \frac{\partial}{\partial x} b_e \\ 0 & 0 \end{pmatrix}, \begin{pmatrix} 0 & 0 \\ -\frac{\partial}{\partial y} b_e & \frac{\partial}{\partial x} b_e \end{pmatrix} \right\}, \tag{37}$$

where $\mathcal{P}_1(\mathcal{B}_e)$ denotes the space of polynomials of degree ≤ 1 on $\mathcal{B}_e$. The discretized displacements are linearized rigid body motions,

$$\mathcal{L}_h := \{\mathbf{v} \in \mathbf{L}_2(\mathcal{B}) : \mathbf{v}\,|_{\mathcal{B}_e} = (a,b) + c(-y,x);\ a,b,c \in \mathbb{R} \quad \forall e\} \tag{38}$$

and for the rotations γ we define

$$\mathcal{W}_h := \{\theta \in L_2(\mathcal{B}) : \theta|_{\mathcal{B}_e} \in \mathcal{P}_1(\mathcal{B}_e) \quad \forall e\}\,. \tag{39}$$

No interelement continuity is required in the definition of $\mathcal{L}_h$ and $\mathcal{W}_h$. The discretized stresses satisfy the condition $\operatorname{div}\boldsymbol{\sigma}_h \in L_2(\mathcal{B})^2$ if and only if the normal tractions $\boldsymbol{\sigma}_h\mathbf{n}$ are continuous across inner element boundaries. This is the only continuity requirement.

In order to avoid expressing the continuity in the definition of the stress space, a Lagrangian multiplier $\boldsymbol{\lambda}_h$ is introduced which lives on the finite element edges only. This renders a hybrid formulation. It is easily verified that on all edges $\boldsymbol{\sigma}_h\mathbf{n}$ is of polynomial degree one. Thus $\boldsymbol{\lambda}_h$ must be of polynomial degree one in order to enforce continuity exactly. At the vertices there are no continuity requirements for $\boldsymbol{\lambda}_h$. Hence $\boldsymbol{\lambda}_h$ will be in the space

$$\begin{aligned} \mathcal{M}_{h,\bar{u}} := \{\boldsymbol{\mu} :\ & \boldsymbol{\mu}|_{\Gamma^i} \in \mathcal{P}_1(\Gamma^i)^2 \quad \text{for all edges } \Gamma^i, \\ & \boldsymbol{\mu}|_{\Gamma^i} \in \mathbf{P}_{\Gamma^i}(\bar{\mathbf{u}}) \quad \text{if } \Gamma^i \subset \Gamma_u\}. \end{aligned}$$

Here $\mathbf{P}_{\Gamma^i}$ is the L_2 projection onto linear polynomials on the edge Γ^i.

Now the discrete space for the stresses is

$$\mathcal{H}_h := \{\boldsymbol{\tau} : \boldsymbol{\tau}|_{\mathcal{B}_e} \in \mathcal{S}(\mathcal{B}_e) \quad \forall e\}. \tag{40}$$

This yields the following discretization of (36) with conforming elements: *Find* $\boldsymbol{\sigma}_h \in \mathcal{H}_h$, $\mathbf{u}_h \in \mathcal{L}_h$, $\gamma_h \in \mathcal{W}_h$ *and* $\boldsymbol{\lambda}_h \in \mathcal{M}_{h,\bar{u}}$ *such that*

$$\begin{aligned} &\int_{\mathcal{B}} \boldsymbol{\tau} : \mathbb{C}^{-1}\boldsymbol{\sigma}_h \,\mathrm{d}\mathcal{B} + \sum_e \int_{\mathcal{B}_e} \operatorname{div}\boldsymbol{\tau}\cdot\mathbf{u}_h \,\mathrm{d}\mathcal{B} \\ &\qquad + \int_{\mathcal{B}} \operatorname{as}(\boldsymbol{\tau})\,\gamma_h \,\mathrm{d}\mathcal{B} - \sum_e \int_{\partial\mathcal{B}_e} \boldsymbol{\tau}\mathbf{n}\cdot\boldsymbol{\lambda}_h \,\mathrm{d}s = 0 && \forall \boldsymbol{\tau} \in \mathcal{H}_h\,, \\ &\sum_e \int_{\mathcal{B}_e} \operatorname{div}\boldsymbol{\sigma}_h\cdot\mathbf{v}\,\mathrm{d}\mathcal{B} = -\int_{\mathcal{B}} \mathbf{f}\cdot\mathbf{v}\,\mathrm{d}\mathcal{B} && \forall \mathbf{v} \in \mathcal{L}_h\,, \\ &\int_{\mathcal{B}} \operatorname{as}(\boldsymbol{\sigma}_h)\,\theta\,\mathrm{d}\mathcal{B} = 0 && \forall \theta \in \mathcal{W}_h\,, \\ &-\sum_e \int_{\partial\mathcal{B}_e} \boldsymbol{\sigma}_h\mathbf{n}\cdot\boldsymbol{\mu}\,\mathrm{d}s = -\int_{\Gamma_t} \bar{\mathbf{t}}\cdot\boldsymbol{\mu}\,\mathrm{d}s && \forall \boldsymbol{\mu} \in \mathcal{M}_{h,0}\,. \end{aligned}$$

Note that in $\sum_e \int_{\partial\mathcal{B}_e} \boldsymbol{\tau}\mathbf{n}\cdot\boldsymbol{\lambda}_h\,\mathrm{d}s$ all interior edges occur twice, but with $\mathbf{n}$ in opposite direction. The last equation ensures the continuity of $\boldsymbol{\sigma}_h\mathbf{n}$.

The trial spaces satisfy the so-called equilibrium condition: If $\boldsymbol{\sigma}_h \in \mathcal{H}_h$ satisfies the conditions $\operatorname{div} \boldsymbol{\sigma}_h \in L_2(\mathcal{B})^2$ and

$$\int_{\mathcal{B}_e} \operatorname{div} \boldsymbol{\sigma}_h \cdot \mathbf{v}_h \, \mathrm{d}\mathcal{B} = 0 \quad \forall \mathbf{v}_h \in \mathcal{L}_h \tag{41}$$

then there holds $\operatorname{div} \boldsymbol{\sigma}_h = \mathbf{0}$, see Stenberg [29]. In particular, for vanishing body loads $\mathbf{f} = \mathbf{0}$ the computed stresses satisfy $\operatorname{div} \boldsymbol{\sigma}_h = \mathbf{0}$. This reveals a relationship with the Trefftz idea. However, the method is by no means restricted to the case $\mathbf{f} = \mathbf{0}$.

Concerning a proof of convergence (Stenberg [29]) we remark that the inf–sup condition can be shown to hold for patches of elements; this implies global stability in mesh-dependent norms. A mechanical interpretation of the stability conditions was given by Stein and Rolfes [28]. Using these elements there is no locking as Poisson's ratio ν approaches 0.5.

Since there are no continuity requirements for $\boldsymbol{\sigma}_h$, $\mathbf{u}_h$ and γ_h, the $15+3+3=21$ corresponding degrees of freedom can be eliminated on each element before assembling the global system. This leads to element stiffness matrices which are similar to the standard finite element case since $\boldsymbol{\lambda}_h$ approximates the displacements. It is possible to incorporate the mixed finite element into existing FEM software as a triangle with two nodes on each side (e.g. at the two Gauss–Legendre points) and no nodes at the vertices. Since we are dealing with straight-sided triangles, no numerical integration is necessary and most work can be done analytically. However, it is not possible to implement the element in a purely isoparametric fashion. A detailed description of the implementation and numerical results can be found in Ref. [17]. *A posteriori* error estimators are discussed in References [3] and [5]. An extension to three-dimensional problems is possible [29].

4. Coupling of BEM and dual mixed FEM

In this section we are going to present a canonical coupling of dual mixed FEM and Galerkin–BEM. The benefit of a Bubnov–Galerkin method is that the matrices are symmetric and the method is easier to analyze mathematically [9, 11]. For collocation (also discussed in [6]) the analysis is still unsatisfactory [7]. As will be seen, our coupling is in a sense 'dual' to Costabel's coupling [9, 11] since we cannot insert the traces of the displacements in the FEM domain into the boundary integral equations. Our method and the analysis in [4] answer some questions arising from general coupled formulations such as those proposed by Polizzotto and Zito [23]. An extension of our method to nonlinear behaviour in the FEM-domain was addressed recently by Gatica and Wendland [12].

A coupling with other types of Trefftz elements could be investigated in the macro-element framework given by Wendland [32].

We consider the linear elasticity problem

$$\left.\begin{array}{lll} \operatorname{div} \boldsymbol{\sigma} = -\mathbf{f} & \text{in} & \mathcal{B}_F \cup \Gamma_C \cup \mathcal{B}_B \\ \mathbb{C}^{-1} \boldsymbol{\sigma} - \boldsymbol{\varepsilon}(\mathbf{u}) = \mathbf{0} & \text{in} & \mathcal{B}_F \cup \Gamma_C \cup \mathcal{B}_B \\ \mathbf{u} = \mathbf{0} & \text{on} & \Gamma_{F_u} \cup \Gamma_u \\ \boldsymbol{\sigma}\mathbf{n} = \bar{\mathbf{t}} & \text{on} & \Gamma_{F_t} \cup \Gamma_t \end{array}\right\} . \tag{42}$$

The domain $\mathcal{B}$ is partitioned into $\mathcal{B} = \mathcal{B}_F \cup \Gamma_C \cup \mathcal{B}_B$ (see Figure 4). The subdomain which is treated by the boundary element method is denoted by $\mathcal{B}_B$ and is assumed to be connected. Its boundary is $\Gamma_B = \Gamma_u \cup \Gamma_t \cup \Gamma_C$. In $\mathcal{B}_F$ a mixed finite element method is employed. We assume that the body load $\mathbf{f}$ vanishes on $\mathcal{B}_B$ and that the Lamé coefficients are constant on $\mathcal{B}_B$.

4.1. Variational formulation of the coupling

In analogy to (36) the weak formulation in $\mathcal{B}_F$ is

$$\int_{\mathcal{B}_F} \boldsymbol{\tau} : \mathbb{C}^{-1} \boldsymbol{\sigma} \, \mathrm{d}\mathcal{B} + \int_{\mathcal{B}_F} \operatorname{div} \boldsymbol{\tau} \cdot \mathbf{u} \, \mathrm{d}\mathcal{B} + \int_{\mathcal{B}_F} \operatorname{as}(\boldsymbol{\tau}) \, \gamma \, \mathrm{d}\mathcal{B} = \int_{\Gamma_C} \boldsymbol{\tau}\mathbf{n} \cdot \mathbf{u} \, \mathrm{d}s \qquad \forall \boldsymbol{\tau},$$

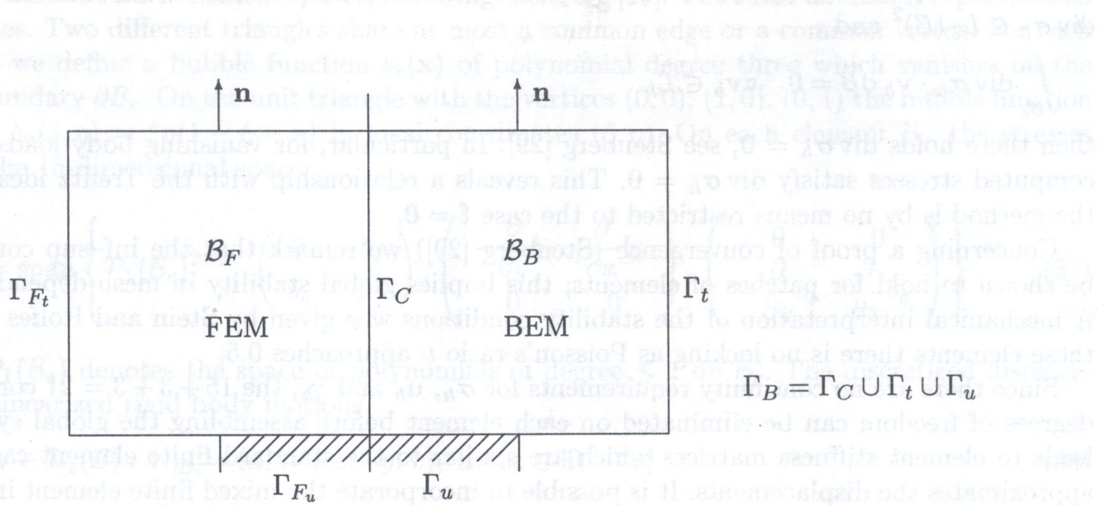

Fig. 4. Notation

$$\int_{\mathcal{B}_F} \operatorname{div} \boldsymbol{\sigma} \cdot \mathbf{v} \, d\mathcal{B} = -\int_{\mathcal{B}_F} \mathbf{f} \cdot \mathbf{v} \, d\mathcal{B} \qquad \forall \mathbf{v},$$
$$\int_{\mathcal{B}_F} \operatorname{as}(\boldsymbol{\sigma}) \, \theta \, d\mathcal{B} = 0 \qquad \forall \theta. \tag{43}$$

To derive the coupled scheme, the first step is to introduce a new variable $\boldsymbol{\varphi} := \mathbf{u}|_{\Gamma_B}$ in the trace space

$$\mathbf{H}^{1/2} := \left\{ \boldsymbol{\psi} \in H^{1/2}(\Gamma_B)^2 : \boldsymbol{\psi} = \mathbf{0} \quad \text{on} \quad \Gamma_u \right\} \tag{44}$$

For the tractions $\mathbf{t}$ on the boundary of the BEM domain we require equilibrium across the FEM–BEM interface, more specifically

$$\begin{aligned} (\boldsymbol{\sigma}, \mathbf{t}) \in \; & \left\{ (\boldsymbol{\tau}, \boldsymbol{\chi}) \in \mathbf{H}(\operatorname{div}, \mathcal{B}_F) \times H^{-1/2}(\Gamma_B)^2 : \right. \\ & \left. \boldsymbol{\chi} = -\boldsymbol{\tau}\mathbf{n} \quad \text{on} \quad \Gamma_C, \quad \boldsymbol{\chi} = \bar{\mathbf{t}} \quad \text{on} \quad \Gamma_t, \quad \boldsymbol{\tau}\mathbf{n} = \bar{\mathbf{t}} \quad \text{on} \quad \Gamma_{F_t} \right\} \\ & =: \mathcal{H}_{(t)} \times \mathbf{H}^{-1/2}. \end{aligned}$$

For a definition of the underlying Sobolev spaces on polygonal boundaries and basic properties of the integral operators we refer to [10] and [11]. From the first integral equation (5) we know

$$\mathbf{u} = \mathbf{V}\mathbf{t} + \left(\tfrac{1}{2}\mathbf{I} - \mathbf{K}\right) \boldsymbol{\varphi}.$$

This is inserted for $\mathbf{u}|_{\Gamma_C}$ into the right-hand side of the first equation of (43), leading to

$$\int_{\mathcal{B}_F} \boldsymbol{\tau} : \mathbb{C}^{-1} \boldsymbol{\sigma} \, d\mathcal{B} + \int_{\mathcal{B}_F} \operatorname{div} \boldsymbol{\tau} \cdot \mathbf{u} \, d\mathcal{B} + \int_{\mathcal{B}_F} \operatorname{as}(\boldsymbol{\tau}) \, \gamma \, d\mathcal{B} + \langle \boldsymbol{\chi}, \mathbf{V}\mathbf{t} \rangle_{C_u} + \tfrac{1}{2} \langle \boldsymbol{\chi}, \boldsymbol{\varphi} \rangle_C - \langle \boldsymbol{\chi}, \mathbf{K}\boldsymbol{\varphi} \rangle_{C_u} = 0$$

for test functions $(\boldsymbol{\tau}, \boldsymbol{\chi}) \in \mathcal{H}_{(0)} \times \mathbf{H}^{-1/2}$. Here we used the notation $\langle \boldsymbol{\chi}, \boldsymbol{\varphi} \rangle_{C_u} = \int_{\Gamma_C} \boldsymbol{\chi} \cdot \boldsymbol{\varphi} ds$, $\langle , \rangle_{C_u} := \int_{\Gamma_C \cup \Gamma_u} ds$. Note that the first integral equation is applied on $\Gamma_C \cup \Gamma_u$ where the tractions are unknown, while the second integral equation (6) will be exploited on $\Gamma_C \cup \Gamma_t$ where the displacements are unknown. We emphasize that on the interface Γ_C both integral equations are used in order to obtain a symmetric coupling procedure. We introduce some notation by writing

$$\begin{aligned} (\mathbf{V}\mathbf{t})(\mathbf{x}) &= \int_{\Gamma_C \cup \Gamma_u} \mathbf{G}(\mathbf{x}, \mathbf{y}) \, \mathbf{t}(\mathbf{y}) \, ds(\mathbf{y}) + \int_{\Gamma_t} \mathbf{G}(\mathbf{x}, \mathbf{y}) \, \mathbf{t}(\mathbf{y}) \, ds(\mathbf{y}) \\ &=: (\mathbf{V}_{C_u}\mathbf{t})(\mathbf{x}) + (\mathbf{V}_t\mathbf{t})(\mathbf{x}), \end{aligned}$$

and treat the other boundary integral operators similarly.

Now the weak formulation of the coupled problem reads: Find

$$(\boldsymbol{\sigma}, \mathbf{t}, \boldsymbol{\varphi}, \mathbf{u}, \gamma) \in \mathcal{H}_{(\bar{t})} \times \mathbf{H}^{-1/2} \times \mathbf{H}^{1/2} \times \mathbf{L}_2(\mathcal{B}_F) \times L_2(\mathcal{B}_F)$$

such that

$$\left.\begin{aligned} a(\boldsymbol{\sigma}, \mathbf{t}, \boldsymbol{\varphi}; \boldsymbol{\tau}, \boldsymbol{\chi}, \boldsymbol{\psi}) + b(\boldsymbol{\tau}; \mathbf{u}, \gamma) &= l(\boldsymbol{\chi}, \boldsymbol{\psi}), \\ b(\boldsymbol{\sigma}; \mathbf{v}, \theta) &= -\int_{\mathcal{B}_F} \mathbf{f} \cdot \mathbf{v} \, d\mathcal{B} \end{aligned}\right\} \qquad (45)$$

for all $(\boldsymbol{\tau}, \boldsymbol{\chi}, \boldsymbol{\psi}, \mathbf{v}, \theta) \in \mathcal{H}_{(0)} \times \mathbf{H}^{-1/2} \times \mathbf{H}^{1/2} \times \mathbf{L}_2(\mathcal{B}_F) \times L_2(\mathcal{B}_F)$. The bilinear forms a and b are defined as

$$\begin{aligned} a(\boldsymbol{\sigma}, \mathbf{t}, \boldsymbol{\varphi}; \boldsymbol{\tau}, \boldsymbol{\chi}, \boldsymbol{\psi}) = & \int_{\mathcal{B}_F} \boldsymbol{\tau} : \mathbb{C}^{-1} \boldsymbol{\sigma} \, d\mathcal{B} \\ & + \langle \boldsymbol{\chi}, \mathbf{V}_{C_u} \mathbf{t} \rangle_{C_u} + \tfrac{1}{2} \langle \boldsymbol{\chi}, \boldsymbol{\varphi} \rangle_C - \langle \boldsymbol{\chi}, \mathbf{K}_{C_t} \boldsymbol{\varphi} \rangle_{C_u} \\ & + \langle \boldsymbol{\psi}, \mathbf{W}_{C_t} \boldsymbol{\varphi} \rangle_{C_t} + \tfrac{1}{2} \langle \boldsymbol{\psi}, \mathbf{t} \rangle_C - \langle \boldsymbol{\psi}, \mathbf{K}'_{C_u} \mathbf{t} \rangle_{C_t} \end{aligned}$$

and

$$b(\boldsymbol{\sigma}; \mathbf{v}, \theta) = \int_{\mathcal{B}_F} \operatorname{div} \boldsymbol{\sigma} \cdot \mathbf{v} \, d\mathcal{B} + \int_{\mathcal{B}_F} \operatorname{as}(\boldsymbol{\sigma}) \, \theta \, d\mathcal{B}$$

and the linear form l on the right-hand side is

$$l(\boldsymbol{\chi}, \boldsymbol{\psi}) = -\langle \boldsymbol{\chi}, \mathbf{V}_t \bar{\mathbf{t}} \rangle_{C_u} - \tfrac{1}{2} \langle \boldsymbol{\psi}, \bar{\mathbf{t}} \rangle_t + \langle \boldsymbol{\psi}, \mathbf{K}'_t \bar{\mathbf{t}} \rangle_{C_t}.$$

Note that the bilinear form a is symmetric, i.e.

$$a(\boldsymbol{\sigma}, \mathbf{t}, \boldsymbol{\varphi}; \boldsymbol{\tau}, \boldsymbol{\chi}, \boldsymbol{\psi}) = a(\boldsymbol{\tau}, \boldsymbol{\chi}, \boldsymbol{\psi}; \boldsymbol{\sigma}, \mathbf{t}, \boldsymbol{\varphi})$$

since $\mathbb{C}$ is symmetric, the operators $\mathbf{V}$ and $\mathbf{W}$ are selfadjoint and

$$\langle \boldsymbol{\chi}, \mathbf{K}_{C_t} \boldsymbol{\varphi} \rangle_{C_u} = \langle \boldsymbol{\varphi}, \mathbf{K}'_{C_u} \mathbf{t} \rangle_{C_t}.$$

Equation (45) is a typical saddle point problem in the sense of Babuška and Brezzi's theory. Stability and optimal order convergence of the coupled scheme are proved in Ref. [4]

4.2. Discrete formulation with interelement Lagrange multipliers

For the conforming discretization of (45) we use the finite element spaces of Section 3.2. For simplicity, we assume the boundary elements on the interface Γ_C to be edges of finite elements. On $\Gamma_C \cup \Gamma_t$ the trial functions for the displacements are continuous piecewise linear functions, and for the tractions $\mathbf{t}_h$ we use discontinuous piecewise linear functions on $\Gamma_C \cup \Gamma_u$. Again the continuity of the interelement tractions is ensured by a Lagrange multiplier. With the same technique the condition $\mathbf{t}_h = -\boldsymbol{\sigma}_h \mathbf{n}$ on the interface Γ_C is enforced. This hybridization does not change the solution of the discretization of (45).

4.3. Numerical Examples

Numerical results are given for two plane strain problems. The body load $\mathbf{f}$ is disregarded. In Cook's problem (Figure 5), on the right-hand edge the traction $\boldsymbol{\sigma}\mathbf{n} = (0, 1/16)$ is applied while the upper and lower boundary is free of loads. The material parameters are Young's modulus $E = 1$ and Poisson's ratio $\nu = 1/3$ or $\nu = 0.4999$. Each mesh refinement step is performed by halving all finite element sides and all boundary elements.

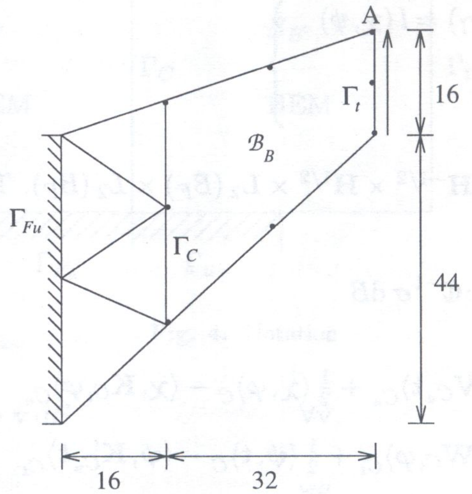

Fig. 5. Example 1, plane strain problem, initial mesh with 4 finite and 8 boundary elements

In Figure 6 the computed vertical displacement at the Point A (see Figure 5) is shown for increasing number of degrees of freedom in the global system, i.e. in the unknowns $\boldsymbol{\lambda}_h$, $\mathbf{t}_h$ and φ_h. The coupled method is compared with three other schemes in which the whole domain is treated by (i) the mixed FEM, (ii) the symmetric Galerkin BEM, and (iii) standard triangular P2 finite elements, i.e., with trial functions for the displacements only, having polynomial degree two. Computed displacements were compared at other points also, showing that the BEM needs the lowest number of degrees of freedom while the other methods lead to approximately the same accuracy. However, the BEM matrices are fully populated.

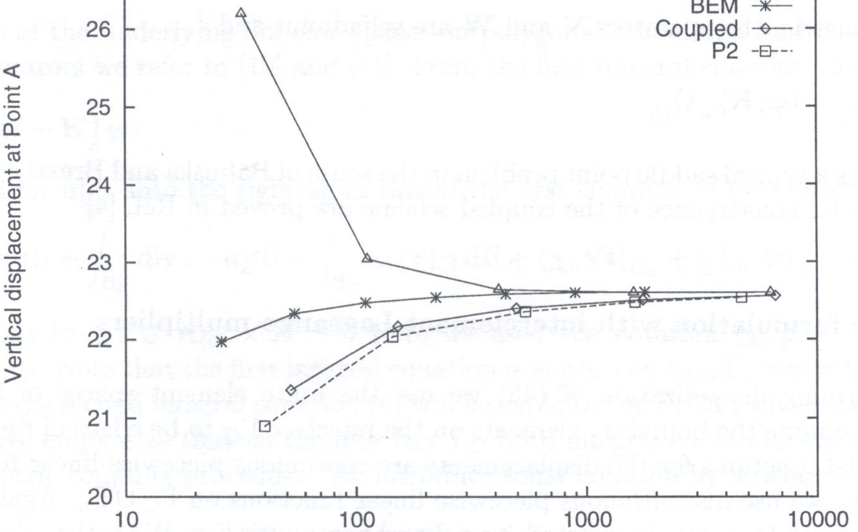

Fig. 6. Example 1, displacement for $\nu = 1/3$

Figure 7 shows the corresponding results for the almost incompressible case. Now the P2-element is clearly less efficient than the other methods. This locking phenomenon is even worse when employing the standard bilinear element, which, for this bending dominated problem, yields unacceptable results. For a comparison with other mixed finite element methods we refer to [17].

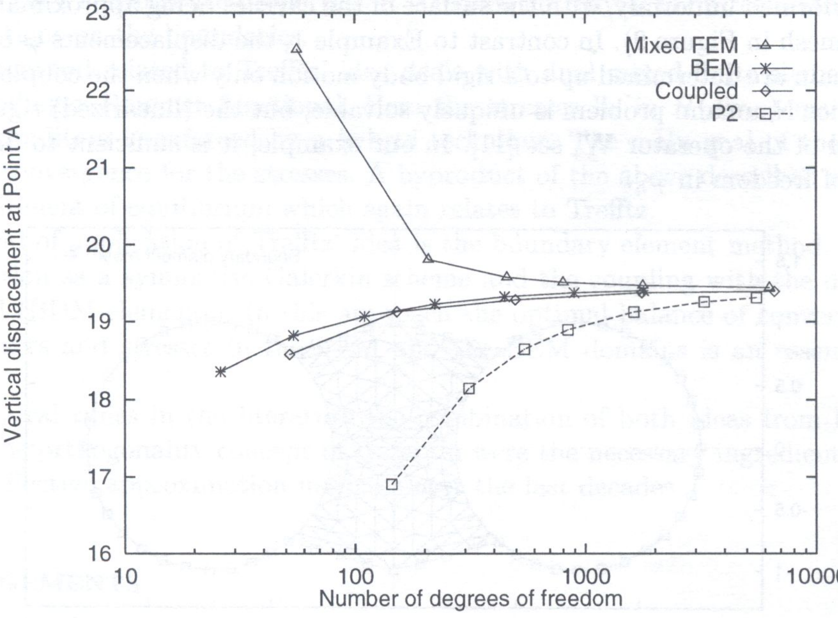

Fig. 7. Example 1, displacement for $\nu = 0.4999$

In Figure 8 the normal stress σ_{11} at the left-hand boundary (Γ_{Fu} in Figure 5) is depicted. For all methods, meshes with eight elements on the left-hand boundary were used. Except near the corners (where singularities are present), the results are almost indistinguishable.

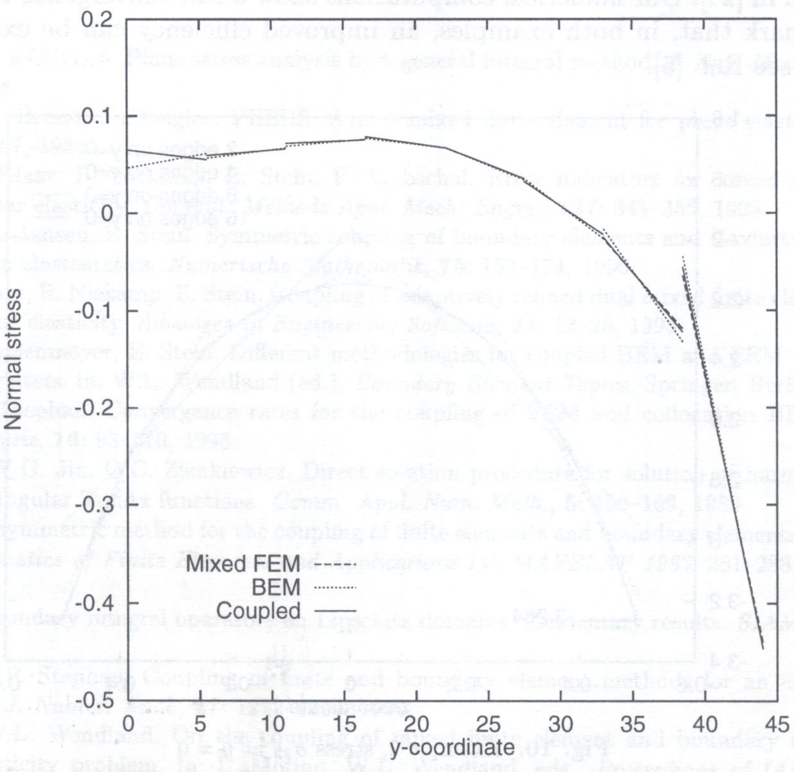

Fig. 8. Example 1, normal stress at left-hand boundary for $\nu = 0.4999$

For this simple model problem, the coupling does not have an advantage over the other methods, but the computations show that the mixed element and the BEM suit well to each other.

In the second example we consider two neighboring cylindrical cavities in an unbounded medium under uniform vertical pressure of magnitude 1. For the radius R of the cavities and the distance l between them we take $R = l = 1$. The material parameters are $E = 1$ and $\nu = 0.2$. The mesh refinement is performed uniformly, with the surface of the cavities being approximated by piecewise linears (see the mesh in Figure 9). In contrast to Example 1, the displacements φ on the boundary of the BEM domain are determined up to a rigid body motion only when the coupled formulation is used. This exterior Neumann problem is uniquely solvable, but the (linearized) rigid body motions are in the kernel of the operator $\mathbf{W}$, see [11]. In our example, it is sufficient to fix three suitably chosen degrees of freedom in φ_h.

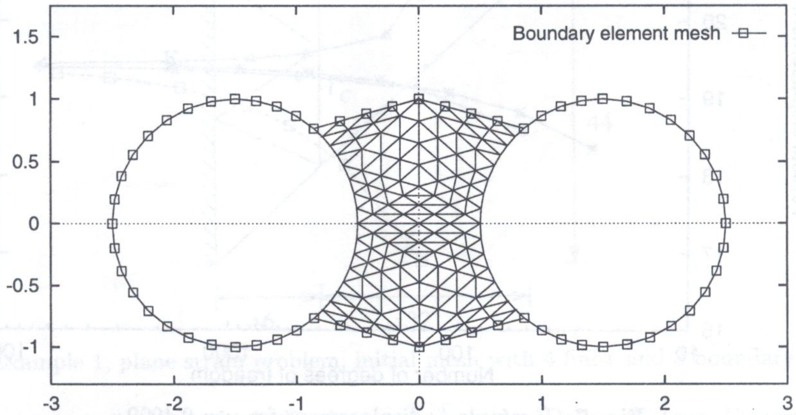

Fig. 9. Example 2, unbounded medium under vertical pressure with two cavities, plane strain, mesh with 224 finite elements and 64 boundary elements

Figure 10 shows the normal stress σ_{22} on the horizontal line $y = 0$ in the FEM domain. The largest stress occurs at the boundary of the cavities and has the value -3.264 according to the analytical solution in [24]. Our numerical computations show a fast convergence towards this value.

Finally we remark that, in both examples, an improved efficiency can be expected from local mesh refinement, see Ref. [5].

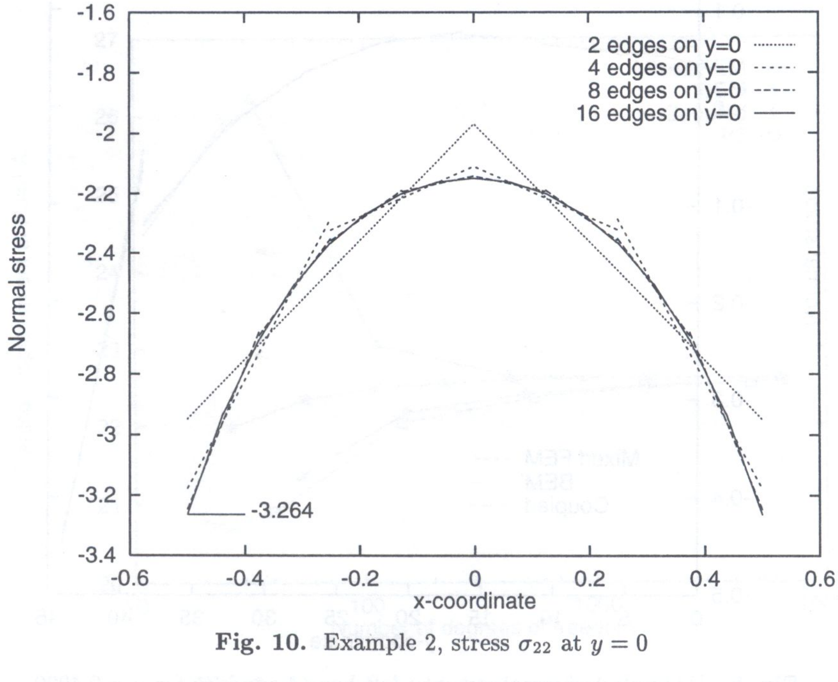

Fig. 10. Example 2, stress σ_{22} at $y = 0$

5. Conclusions

Three applications and extensions of Trefftz' method are treated in this paper, first boundary-type elements based on Beltrami stress functions, fulfilling the field equations. As can be seen from Table 1, different regularizations of consistency and stability conditions were treated and tested, exhibiting fairly good convergence properties. It is indeed not trivial to overcome the nonconformity of the trial functions on the boundaries.

The second method related to Trefftz' idea deals with dual mixed finite elements arising from an extended Hellinger–Reissner functional. Here the stresses lie in $H(\mathrm{div},.)$-spaces, and computationally this condition is enforced by a hybrid technique. The main goal of these elements is a higher order of convergence for the stresses. A byproduct of the above described mixed element is the a-priori fulfillment of equilibrium which again relates to Trefftz.

The third field of application of Trefftz' idea is the boundary element method. Here we considered the realization as a symmetric Galerkin scheme and the coupling with the dual mixed finite element method (BDM-elements). In this approach the optimal balance of convergence orders for both displacements and stresses in the FEM and the BEM domains is an essential goal of this contribution.

As stated several times in the literature the combination of both ideas from Ritz and Trefftz and especially the orthogonality concept of Galerkin were the necessary ingredients for developing consistent and effective approximation methods over the last decades.

Acknowledgements

We are indebted to Dr. M. Maischak, Hannover, for lending us subroutines to compute the BEM integrals. Parts of this research were supported by the German Research Foundation (DFG) within the Priority Research Program 'Boundary Element Methods' under Grant No. Ste 238/19-3.

References

[1] E.R. de Arantes e Oliviera. Plane stress analysis by a general integral method. *J. Eng. Mech. Div., Proc. ASCE*, **94**: 79–101, 1968.

[2] D.N. Arnold, F. Brezzi, J. Douglas. PEERS: A new mixed finite element for plane elasticity. *Japan J. Appl. Math.*, **1**: 347–367, 1984.

[3] D. Braess, O. Klaas, R. Niekamp, E. Stein, F. Wobschal. Error indicators for mixed finite elements in 2-dimensional linear elasticity. *Comput. Methods Appl. Mech. Engrg.*, **127**: 345–356, 1995.

[4] U. Brink, C. Carstensen, E. Stein. Symmetric coupling of boundary elements and Raviart–Thomas-type mixed finite elements in elastostatics. *Numerische Mathematik*, **75**: 153–174, 1996.

[5] U. Brink, O. Klaas, R. Niekamp, E. Stein. Coupling of adaptively refined dual mixed finite elements and boundary elements in linear elasticity. *Advances in Engineering Software*, **24**: 13–26, 1995.

[6] U. Brink, M. Kreienmeyer, E. Stein. Different methodologies for coupled BEM and FEM with implementation on parallel computers. in: W.L. Wendland (ed.), *Boundary Element Topics*, Springer, Berlin, 1996, to appear.

[7] U. Brink, E.P. Stephan. Convergence rates for the coupling of FEM and collocation BEM. *IMA Journal of Numerical Analysis*, **16**: 93–110, 1996.

[8] Y.K. Cheung, W.G. Jin, O.C. Zienkiewicz. Direct solution procedure for solution of harmonic problems using complete, non-singular Trefftz functions. *Comm. Appl. Num. Meth.*, **5**: 159–169, 1989.

[9] M. Costabel. A symmetric method for the coupling of finite elements and boundary elements. In: J.R. Whiteman, ed., *The Mathematics of Finite Elements and Applications IV, MAFELAP 1987*, 281–288. Academic, London, 1988.

[10] M. Costabel. Boundary integral operators on Lipschitz domains: Elementary results. *SIAM J. Math. Anal.*, **19**: 613–626, 1988.

[11] M. Costabel, E.P. Stephan. Coupling of finite and boundary element methods for an elastoplastic interface problem. *SIAM J. Numer. Anal.*, **27**: 1212–1226, 1990.

[12] G.N. Gatica, W.L. Wendland. On the coupling of mixed finite element and boundary integral methods for a nonlinear elasticity problem. In: L. Morino, W.L. Wendland, eds., *Proceedings of IABEM Symposium on Boundary Integral Methods for Nonlinear Problems*, Siena 1995, Kluver, Dordrecht, 1997.

[13] I. Herrera. An algebraic theory of boundary value problems. *KINAM*, **3**(2): 161–230, 1981.

[14] W.G. Jin, Y.K, Cheung, O.C. Zienkiewicz. Application of the Trefftz method in plane elasticity problems. *Int. J. Numer. Meth. Eng.*, **30**: 1147–1161, 1990.

[15] J. Jirousek. The hybrid-Trefftz finite element model and its application to plate bending. *Int. J. Numer. Meth. Eng.*, **23**: 651–693, 1986.

[16] E. Kita, N. Kamiya. Trefftz method: an overview. *Advances in Engineering Software*, **24**: 3–12, 1995.

[17] O. Klaas, J. Schröder, E. Stein, C. Miehe. A regularized dual mixed element for plane elasticity — Implementation and performance of the BDM-Element. *Comput. Methods Appl. Mech. Engrg.*, **121**: 201–209, 1995.

[18] V. D. Kupradze. Potential Methods in the Theory of Elasticity. *Israel Program for Scientific Translations*, 1965.

[19] C. Patterson, M.A. Sheikh. On the use of fundamental solutions in the Trefftz method for potential and elasticity problems. In: C.A. Brebbia, ed., *Boundary Element Methods in Engineering*, 973–980. Springer, Berlin, 1982.

[20] K. Peters, E. Stein, W. Wagner. A new boundary-type finite element for 2-D and 3-D elastic structures. *Int. J. Numer. Meth. Eng.*, **37**: 1009–1025, 1994.

[21] T.H.H. Pian. Derivation of element stiffness matrices by assumed stress distributions. *AIAA J.*, **2**: 1333–1336, 1964.

[22] R. Piltner. Recent developments in the Trefftz method for finite element and boundary element applications. *Advances in Engineering Software*, **24**: 107–115, 1995.

[23] C. Polizzotto, M. Zito. Variational formulations for coupled BE/FE methods in elastostatics. *ZAMM Z. angew. Math. Mech.*, **74**: 533–543, 1994.

[24] G.N. Sawin. *Spannungserhöhung am Rande von Löchern.* VEB Verlag Technik, Berlin, 1956.

[25] E. Stein. *Beiträge zu den direkten Variationsverfahren in der Elastostatik der Balken- und Flächentragwerke.* Doctoral Thesis, Universität Stuttgart, 1964.

[26] E. Stein. Die Kombination des modifizierten Trefftz'schen Verfahrens mit der Methode der finiten Elemente. In: K.E. Buck, D.W. Scharpf, E. Stein, eds., *Finite Elemente in der Statik*, 172–185 and (with Ruoff) 242–259. Verlag W. Ernst & Sohn, Berlin, 1973.

[27] E. Stein, S. Ohnimus. Equilibrium method for postprocessing and error estimation in the Finite Element Method. (also in this volume).

[28] E. Stein, R. Rolfes. Mechanical conditions for stability and optimal convergence of mixed finite elements for linear plane elasticity. *Comput. Methods Appl. Mech. Engrg.*, **84**: 77–95, 1990.

[29] R. Stenberg. A family of mixed finite elements for the elasticity problem. *Numer. Math.*, **53**: 513–538, 1988.

[30] E. Trefftz. Ein Gegenstück zum Ritzschen Verfahren. In: *Verhandlungen des 2. internationalen Kongresses für technische Mechanik*, 131–137. Zürich, 1926.

[31] P. Weidner. *Eine Variante des Trefftzschen Verfahrens zur Lösung der Bipotentialgleichung.* Doctoral Thesis, Universität des Saarlandes, Saarbrücken, 1967.

[32] W.L. Wendland. On the coupling of finite elements and boundary elements. In: G. Kuhn, H. Mang, eds., *Discretization Methods in Structural Mechanics*, 405–414. IUTAM/IACM Symposium Vienna 1989, Springer, Berlin, 1990.

[33] A.P. Zielinski, O.C. Zienkiewicz. Generalized finite element analysis with T-complete boundary solution functions. *Int. J. Numer. Meth. Eng.*, **21**: 509–528, 1985.